Methyl Nitrate, its Molecular *g*-Values, Magnetic Susceptibility Anisotropies, Molecular Electric Quadrupole Moment, Second Moments of the Electronic Charge Distribution, and Electric Field Gradient at the Nitrogen Nucleus

J. Spieckermann and D. H. Sutter

Abteilung Chemische Physik im Institut für Physikalische Chemie
der Christian-Albrechts-Universität zu Kiel

Z. Naturforsch. **44a**, 1087–1096 (1989); received August 12, 1989

The high field molecular Zeeman effect of low-*J* rotational transitions has been observed in methyl nitrate. The spectrum is complicated by the presence of the small ^{14}N nuclear quadrupole coupling. Methyl top internal rotating splitting is negligible in the transitions studied here. From line shape analyses the individual satellite frequencies in the Zeeman-hfs-multiplets could be determined with experimental uncertainties typically smaller than ± 2 kHz. The molecular Zeeman parameters and the ^{14}N nitrogen coupling constants were fitted simultaneously to the observed splittings. The molecular *g*-values are $g_{aa} = -0.1168(5)$, $g_{bb} = -0.0449(3)$, and $g_{cc} = -0.0235(4)$. The molecular magnetic susceptibility anisotropies in units of 10^{-6} erg gauss^{-2} mol^{-1} are $2\xi_{aa} - \xi_{bb} - \xi_{cc} = +1.24(54)$ and $2\xi_{bb} - \xi_{cc} - \xi_{aa} = +13.14(53)$. The ^{14}N nuclear quadrupole coupling constants are $\chi_{aa} = +0.308(17)$ MHz, $\chi_{bb} - \chi_{cc} = -0.262(31)$ MHz. The molecular electric quadrupole moments calculated from the observed rotational constants and Zeeman parameters in units of 10^{-26} esu cm^2 are $Q_{aa} = +3.4(6)$, $Q_{bb} = -4.6(6)$, and $Q_{cc} = +1.2(10)$. Knowledge of the molecular structure and the molecular *g*-values also gives the diagonal elements in the paramagnetic susceptibility tensor and the ansiotropies in the second moments of the electronic charge distribution. The results in units of 10^{-6} erg gauss^{-2} mole^{-1} are $\xi^{\mathrm{p}}_{aa} = +118.14(10)$, $\xi^{\mathrm{p}}_{bb} = +279.73(14)$, and $\xi^{\mathrm{p}}_{cc} = +357.40(26)$, and $\langle a^2 \rangle - \langle b^2 \rangle = +37.14(14)$ Å^2, $\langle b^2 \rangle - \langle c^2 \rangle = +20.46(22)$ Å^2, and $\langle c^2 \rangle - \langle a^2 \rangle = -57.60(21)$ Å^2.

Introduction

We have initiated the present study in view of our interest in local rules for the molecular magnetic susceptibility tensor, here especially of the nitro group, and in substituent effects on the intramolecular electric field gradient at the ^{14}N nucleus. From the earlier studies of Dixon and Wilson [1] and of Cox and Waring [2] methyl nitrate is known to have a planar heavy atom skeleton with the structure shown in Figure 1. Also shown in Fig. 1 is the orientation of the molecular electric dipole moment as determined from Stark effect measurements [2]. In principle the rotational spectrum of methyl nitrate should consist of multiplets split by ^{14}N quadrupole coupling and by methyl top internal rotation but for low-*J* transitions in the torsional ground state neither ^{14}N hyperfine splitting nor internal rotation splitting could be observed in the previous investigations. With a methyl top internal rotation barrier $V_3 = +2321$ cal/mole [1, 3] we indeed could calculate the internal rotation splitting for the observed *a*-type transition to be at most 12 kHz [4]. On the other hand extrapolation from our ^{14}N quadrupole tensor determined for nitric acid [5] indicated that the ^{14}N hfs splittings should be measurable, especially in uncoupled molecular Zeeman effect spectra.

In parallel to the microwave studies, extensive ab initio calculations aiming at the equilibrium structures, the second moments of the electronic charge distribution and at the electric field gradient at the ^{14}N nucleus were carried out by M. H. Palmer [20]. A triple zeta basis of gaussian type orbitals for (C, N, O/H) containing a (10 s 6 p 1 d/5 s 1 p) set contracted to (5 s 3 p 1 d/3 s 1 p) was used in these calculations.

Experimental

The sample was prepared in small quantities by direct esterification from methanol and nitric acid in the presence of sulfuric acid as described by Black and Babers [6]. Great care was taken in the handling of the sample because of its reported explosiveness.

The spectra were recorded with a CW-Stark-spectrometer using 8.3 kHz Stark-modulation and phase stabilized backward wave oscillators as radiation sources. Frequency sweeps were digitally controlled

---

Reprint requests to Prof. Dr. D. H. Sutter, Abteilung Chemische Physik im Institut für Physikalische Chemie der Universität Kiel, Olshausenstr. 40, D-2300 Kiel, West-Germany.

0932-0784 / 89 / 1100-1087 $ 01.30/0. – Please order a reprint rather than making your own copy.

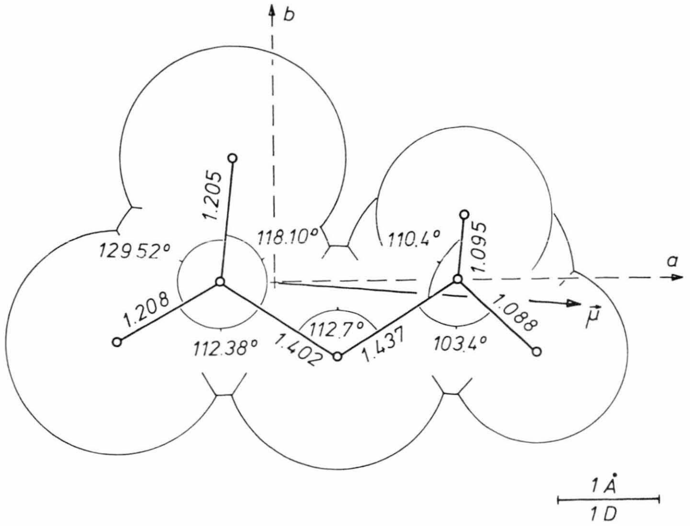

Fig. 1. Microwave substitution structure and electric dipole moment vector of methyl nitrate as determined earlier by Cox and Waring [2]. This structure is used below to derive the second moments of the electron charge distribution from the Zeeman parameters.

by a microcomputer [7]. Oversized rectangular brass waveguide cells were used as absorption cells; an S-band cell with inner cross section of 3.4 cm by 7.2 cm for the $\Delta M_J = 0$ recordings (see below) and a cell with inner cross section of 1.0 cm by 4.7 cm for the $\Delta M_J = \pm 1$ recordings. Furthermore a flow system was used with sample pressures close to 1 mTorr at the entrance hole to the cell and well below 1 mTorr at the exit slit. Under these conditions predominantly Lorentzian line profiles were observed with half widths at half height in the range of 90 to 150 kHz.

Analysis

In zero field the low-J transitions studied here appear as slightly broadened singlets. As mentioned already, the extra broadening is caused by unresolved ^{14}N quadrupole hyperfine splitting and to a much lesser extent by internal rotation splitting. Application of a strong magnetic field however pulls the (M_J, M_I)-satellites apart by the molecular Zeeman effect [8] and leads to at least partly resolved multiplets. The effective Hamiltonian which is appropriate for the analysis of these multiplets is given in symbolic form by

$$\hat{\mathscr{H}}_{\text{eff}} = \hat{\mathscr{H}}_{\text{rot}} + \hat{\mathscr{H}}_{nz} + \hat{\mathscr{H}}_{\text{g}} + \hat{\mathscr{H}}_{\xi} + \hat{\mathscr{H}}_{\text{nq}}\,, \tag{1}$$

which results from a second order perturbation treatment (see Van Vleck Transformation [9]) within the vibronic states which aimes at the vibronic ground state. For details we refer to the derivations presented by Sutter [10] and by Sutter and Flygare [11]. In (1) $\hat{\mathscr{H}}_{\text{rot}}$ is the rigid rotor Hamiltonian, $\hat{\mathscr{H}}_{\text{nz}}$ the nuclear Zeeman effect of the ^{14}N nucleus, $\hat{\mathscr{H}}_{\text{g}}$ the first order molecular Zeeman effect, $\hat{\mathscr{H}}_{\xi}$ the second order molecular Zeeman effect, and $\hat{\mathscr{H}}_{\text{nq}}$ the orientation dependent potential energy of the ^{14}N nuclear quadrupole moment in the intramolecular Coulomb field. ^{14}N spin rotation interaction and internal rotation are neglected. They contribute too little to the splittings of the satellites with respect to the hypothetical center frequencies as to be detectable. Also neglected for the same reason are the nuclear Zeeman effect and the spin-rotation coupling of the hydrogen nuclei.

Since the strong magnetic field effectively uncouples ^{14}N spin and overall rotation, the uncoupled asymmetric top basis $|J, K_a K_c, M_J, I, M_I\rangle$ is best suited to set up the Hamiltonian. Sutter and Flygare [12] have written the first-order energy in this basis. Their result is

$$\begin{aligned}
&\langle J, K_a K_c, M_J, I, M_I |\, \hat{\mathscr{H}}_{\text{eff}} \,| J, K_a K_c, M_J, I, M_I \rangle \\
&= h\{B_a \langle \hat{J}_a^2 \rangle + B_b \langle \hat{J}_b^2 \rangle + B_c \langle \hat{J}_c^2 \rangle\} - \mu_n g_I M_I H \\
&\quad - \mu_n \{g_{aa} \langle \hat{J}_a^2 \rangle + g_{bb} \langle \hat{J}_b^2 \rangle + g_{cc} \langle \hat{J}_c^2 \rangle\} \frac{M_J H}{J(J+1)} \\
&\quad - \frac{1}{2N_{\text{A}}} \xi H^2 - \frac{H^2}{N_{\text{A}}} \frac{3M_J^2 - J(J+1)}{(2J-1)(2J+3)J(J+1)} \\
&\quad \cdot \{(\xi_{aa} - \xi) \langle \hat{J}_a^2 \rangle + (\xi_{bb} - \xi) \langle \hat{J}_b^2 \rangle + (\xi_{cc} - \xi) \langle \hat{J}_c^2 \rangle\} \\
&\quad + \frac{[3M_J^2 - J(J+1)][3M_I^2 - I(I+1)]}{2J(J+1)(2J+3)(2J-1)\,I(2I-1)} \\
&\quad \cdot h\{\chi_{aa} \langle \hat{J}_a^2 \rangle + \chi_{bb} \langle \hat{J}_b^2 \rangle + \chi_{cc} \langle \hat{J}_c^2 \rangle\}\,.
\end{aligned} \tag{2}$$

Table 1. Asymmetric top expectation values for the squares of the components of the rotational angular momentum. According to the Hellman-Feynman theorem they were calculated as partial derivatives of the rigid rotor energies (see for instance Table 5-4 of Ref. [22]) with respect to the rotational constants.

J	K_a	K_c	$\langle J_a^2\rangle$	$\langle J_b^2\rangle$	$\langle J_c^2\rangle$
0	0	0	0.0000	0.0000	0.0000
1	0	1	0.0000	1.0000	1.0000
1	1	1	1.0000	0.0000	1.0000
1	1	0	1.0000	1.0000	0.0000
2	0	2	0.0200	2.7459	3.2341
2	1	2	1.0000	1.0000	4.0000
2	1	1	1.0000	4.0000	1.0000
2	2	1	4.0000	1.0000	1.0000
2	2	0	3.9800	1.2541	0.7659
3	0	3	0.0942	4.7782	7.1276
3	1	3	1.0112	2.3539	8.6349
3	1	2	1.0143	8.3239	2.6618
3	2	2	4.0000	4.0000	4.0000
3	2	1	3.9058	5.2218	2.8724
3	3	1	8.9888	1.6461	1.3651
3	3	0	8.9857	1.6761	1.3382

The notation used here is as follows. h is Planck's constant. B_a, B_b, and B_c are the rotational constants. $\langle\hat{J}_a^2\rangle$, $\langle\hat{J}_b^2\rangle$, and $\langle\hat{J}_c^2\rangle$ are the asymmetric top expectation values of the squares of the rigid rotor angular momentum components with respect to the molecule fixed axes. They are measured in units of $\hbar^2$ and were calculated from the previously determined rotational contants [2]

$$B_a = 11\,795.00\ \text{MHz}, \quad B_b = 4707.53\ \text{MHz}, \quad B_c = 3438.25\ \text{MHz}$$

by differentation of the asymmetric top energy levels with respect to the rotational constants as described in [8], p. 125. Their values are given in Table 1. μ_n is the nuclear magneton. H is the exterior magnetic field which provides the quantization axis, g_I the ^{14}N nuclear g-factor and M_I the projection quantum number of the ^{14}N spin with respect to the exterior field axis. g_{aa}, g_{bb}, and g_{cc} are the molecular g-values along the principal inertia axes. ξ_{aa}, ξ_{bb}, and ξ_{cc} are the molecular magnetic susceptibilities along the principal inertia axes. $\xi = (\xi_{aa} + \xi_{bb} + \xi_{cc})/3$ is the bulk susceptibility. N_A is Avogadro's number. J and M_J are the quantum numbers of the rotational angular momentum (excluding spin) and of its projection on the magnetic field axis (z-axis). χ_{aa}, χ_{bb}, and χ_{cc} are the ^{14}N quadrupole coupling constants. They are related to the vibronic ground state expectation values of the intramolecular electric field gradient at the ^{14}N nucleus by

$$\chi_{aa} = |e|\, Q \left\langle \frac{\partial^2 V}{\partial a^2} \right\rangle \Big/ h \text{ (and cyclic permutations)} \tag{3}$$

with e the electronic charge and Q the ^{14}N nuclear quadrupole moment. (For the ^{14}N nuclear quadrupole moment Sundholm, Pyykkö, Laaksonen and Sadlej [13] have recently proposed a value of $2.05 \pm 0.05 \cdot 10^{-26}$ cm^2 on the basis of a comparison of their ab initio field gradients with experimental ^{14}N quadrupole coupling constants in NO$^+$ and N$_2$.) All other fundamental constants were taken from Appendix E of [14].

There are also off-diagonal elements of the effective Hamiltonian. From these, all elements which are off-diagonal in the rigid rotor quantum numbers J and $K_a K_c$* can be safely neglected in our present application since they contribute too little. But the ^{14}N quadrupole coupling corrections which are off-diagonal only in M_J and M_I have to be accounted for in a high resolution study as presented here. They have been given by Wang and Flygare [15] and independently by Sutter [10] as

$$\begin{aligned}&\langle J, K_a K_c, M_J \pm 1, I, M_I \mp 1 |\, \mathscr{H}_{\text{nq}} \,| J, K_a K_c, M_J, I, M_I\rangle \\ &\quad = \tfrac{3}{4}\, C (2M_J \pm 1)(2M_I \mp 1) \sqrt{(J \mp M_J)(J \pm M_J + 1)(I \pm M_I)(I \mp M_I + 1)}\end{aligned} \tag{4}$$

and

$$\begin{aligned}&\langle J, K_a K_c, M_J \pm 2, I, M_I \mp 2 |\, \mathscr{H}_{\text{nq}} \,| J, K_a K_c, M_J, I, M_I\rangle \\ &\quad = \tfrac{3}{4}\, C \sqrt{(J \mp M_J)(J \mp M_J - 1)(J \pm M_J + 1)(J \pm M_J + 2)(I \pm M_I)(I \pm M_I - 1)(I \mp M_I + 1)(I \mp M_I + 2)}\end{aligned} \tag{5}$$

with

$$C = \frac{\{\chi_{aa}\langle\hat{J}_a^2\rangle + \chi_{bb}\langle\hat{J}_b^2\rangle + \chi_{cc}\langle\hat{J}_c^2\rangle\}}{I(2I-1)\, J(J+1)(2J-1)(2J+3)}\,. \tag{6}$$

---

* The asymmetric top states are designated by J and the K-quantum numbers of the limiting prolate and oblate symmetric tops, K_a and K_c, respectively.

Table 2. Hypothetic center frequencies (ν_c) and Zeemann-^{14}N-hfs-splittings ($\Delta\nu = \nu - \nu_c$) observed for several low-J rotational transitions of methyl nitrate in its vibronic ground state. (– indicates satellites with low intensity and poor signal to noise ratio not included in the fit, * indicates satellites perturbed by Stark-lobes or other unassigned lines, also not included in the fit.) All frequencies are given in MHz. Relative internsities are in arbitrary units.

$J'\,K'_a\,K'_c - J\,K_a\,K_c$ ν_c	H/Gauss ΔM_J	M_I	M'_J	M_J	Rel. int.	$\Delta\nu_{exp}$	$\Delta\nu_{calc}$	$\Delta\nu_{exp} - \Delta\nu_{calc}$
101 – 000	13 395	−1.0	0	0	2	0.0390	0.0275	0.0115
8 145.793	0	0.0	0	0	2	−0.0503	−0.0655	0.0150
		1.0	0	0	2	0.0390	0.0266	0.0124
211 – 110	13 395	−1.0	−1	−1	6	0.3175	0.3261	−0.0086
17 560.893	0	−1.0	0	0	8	−0.0006	0.0080	−0.0086
		−1.0	1	1	6	−0.2508	−0.2359	−0.0149
		0.0	−1	−1	6	0.2938	0.2989	−0.0051
		0.0	0	0	8	−0.0785	−0.0602	−0.0183
		0.0	1	1	6	−0.2607	−0.2638	0.0031
		1.0	−1	−1	6	0.3175	0.3252	−0.0077
		1.0	0	0	8	−0.0006	0.0073	−0.0079
		1.0	1	1	6	−0.2508	−0.2368	−0.0140
211 – 110	18 086	−1.0	−1	−1	6	0.4505	0.4537	−0.0031
17 560.893	0	−1.0	0	0	8	0.0007	−0.0044	0.0051
		−1.0	1	1	6	−0.3134	−0.3052	−0.0082
		0.0	−1	−1	6	0.4214	0.4266	−0.0052
		0.0	0	0	8	*	−0.0726	*
		0.0	1	1	6	−0.3301	−0.3328	0.0027
		1.0	−1	−1	6	0.4506	0.4531	−0.0025
		1.0	0	0	8	0.0007	−0.0049	0.0056
		1.0	1	1	6	−0.3134	−0.3058	−0.0076
212 – 111	13 395	−1.0	−1	−1	6	0.2427	0.2325	0.0102
15 022.261	0	−1.0	0	0	8	0.0425	0.0383	0.0042
		−1.0	1	1	6	−0.3135	−0.3306	0.0171
		0.0	−1	−1	6	0.2600	0.2731	−0.0131
		0.0	0	0	8	−0.0527	−0.0516	−0.0056
		0.0	1	1	6	−0.3008	−0.2897	−0.0111
		1.0	−1	−1	6	0.2427	0.2337	0.0090
		1.0	0	0	8	0.0425	0.0391	0.0034
		1.0	1	1	6	−0.3135	−0.3295	0.0160
212 – 111	18 086	−1.0	−1	−1	6	0.2924	0.3021	−0.0097
15 022.261	0	−1.0	0	0	8	0.0383	0.0455	−0.0072
		−1.0	1	1	6	−0.4665	−0.4576	−0.0089
		0.0	−1	−1	6	0.3423	0.3426	−0.0003
		0.0	0	0	8	−0.0561	−0.0446	−0.0115
		0.0	1	1	6	−0.4358	−0.4169	−0.0189
		1.0	−1	−1	6	0.2924	0.3029	−0.0105
		1.0	0	0	8	0.0383	0.0460	−0.0077
		1.0	1	1	6	−0.4665	−0.4568	−0.0097
211 – 110	13 395	−1.0	−2	−1	6	−0.2887	−0.2913	0.0026
17 560.863	±1	−1.0	0	−1	1	–	0.8945	–
		−1.0	−1	0	3	−0.5597	−0.5605	0.0008
		−1.0	1	0	3	0.5257	0.5282	−0.0025
		−1.0	0	1	1	–	−0.7561	–
		−1.0	2	1	6	0.2452	0.2359	0.0093
		0.0	−2	−1	6	−0.2104	−0.2272	0.0168
		0.0	0	−1	1	–	0.8366	–
		0.0	−1	0	3	−0.5718	−0.5979	0.0261
		0.0	1	0	3	0.5206	0.4900	0.0306
		0.0	0	1	1	–	−0.8139	–
		0.0	2	1	6	0.3244	0.3000	0.0244
		1.0	−2	−1	6	−0.2887	−0.2919	0.0032
		1.0	0	−1	1	–	0.8938	–
		1.0	−1	0	3	−0.5597	−0.5613	0.0016
		1.0	1	0	3	0.5257	0.5273	−0.0016
		1.0	0	1	1	–	−0.7567	–
		1.0	2	1	6	0.2452	0.2352	0.0100
211 – 110	18 086	−1.0	−2	−1	6	−0.3938	−0.3889	−0.0049
17 560.863	±1	−1.0	0	−1	1	–	1.2243	–
		−1.0	−1	0	3	−0.7831	−0.7751	−0.0080
		−1.0	−1	0	3	−0.6844	0.6947	−0.0103
		−1.0	0	1	1	–	−1.0043	–
		−1.0	2	1	6	0.3225	0.3225	0.0034
		0.0	−2	−1	6	−0.3034	−0.3247	0.0213
		0.0	0	−1	1	–	1.1665	–
		0.0	−1	0	3	−0.8036	−0.8125	0.0089
		0.0	1	0	3	*	0.6567	*
		0.0	0	1	1	–	−1.0602	–
		0.0	2	1	6	*	0.3867	*
		1.0	−2	−1	6	−0.3938	−0.3894	−0.0044
		1.0	0	−1	1	–	1-2238	–
		1.0	−1	0	3	−0.7831	−0.7757	−0.0074
		1.0	1	0	3	0.6844	0.6941	−0.0097
		1.0	0	1	1	–	−1.0047	–
		1.0	2	1	6	0.3259	0.3220	0.0039
212 – 111	13 395	−1.0	−2	−1	6	*	−0.1585	*
15 022.276	±1	−1.0	0	−1	1	–	0.6527	–
		−1.0	−1	0	3	−0.3740	−0.3819	0.0079
		−1.0	1	0	3	0.4959	0.4877	0.0082
		−1.0	0	1	1	–	−0.7800	–
		−1.0	2	1	6	*	0.1479	*
		0.0	−2	−1	6	*	−0.1105	*
		0.0	0	−1	1	–	0.6907	–
		0.0	−1	0	3	−0.4694	−0.4694	0.0129
		0.0	1	0	3	0.3877	0.4002	−0.0125
		0.0	0	1	1	–	−0.7415	–
		0.0	2	1	6	*	0.1962	*
		1.0	−2	−1	6	*	−0.1574	*
		1.0	0	−1	1	–	0.6539	–
		1.0	−1	0	3	−0.3740	−0.3812	0.0072
		1.0	1	0	3	0.4959	0.4885	0.0074
		1.0	0	1	1	–	−0.7789	–
		1.0	2	1	6	*	0.1490	*
212 – 111	18 086	−1.0	−2	−1	6	*	−0.2032	*
15 022.276	±1	−1.0	0	−1	1	–	0.8619	–
		−1.0	−1	0	3	−0.5166	−0.5144	−0.0022
		−1.0	1	0	3	0.6688	0.6598	0.0090
		−1.0	0	1	1	–	−1.0719	–
		−1.0	2	1	6	*	0.2111	*
		0.0	−2	−1	6	*	−0.1553	*
		0.0	0	−1	1	–	0.8999	–
		0.0	−1	0	3	−0.5928	−0.6019	0.0091
		0.0	1	0	3	0.5773	0.5722	0.0051
		0.0	0	1	1	–	−1.0336	–
		0.0	2	1	6	*	0.2593	*
		1.0	−2	−1	6	*	−0.2024	*
		1.0	0	−1	1	–	0.8627	–
		1.0	−1	0	3	−0.5166	−0.5138	−0.0028
		1.0	1	0	3	0.6688	0.6604	0.0084
		1.0	0	1	1	–	−1.0711	–
		1.0	2	1	6	*	0.2120	*

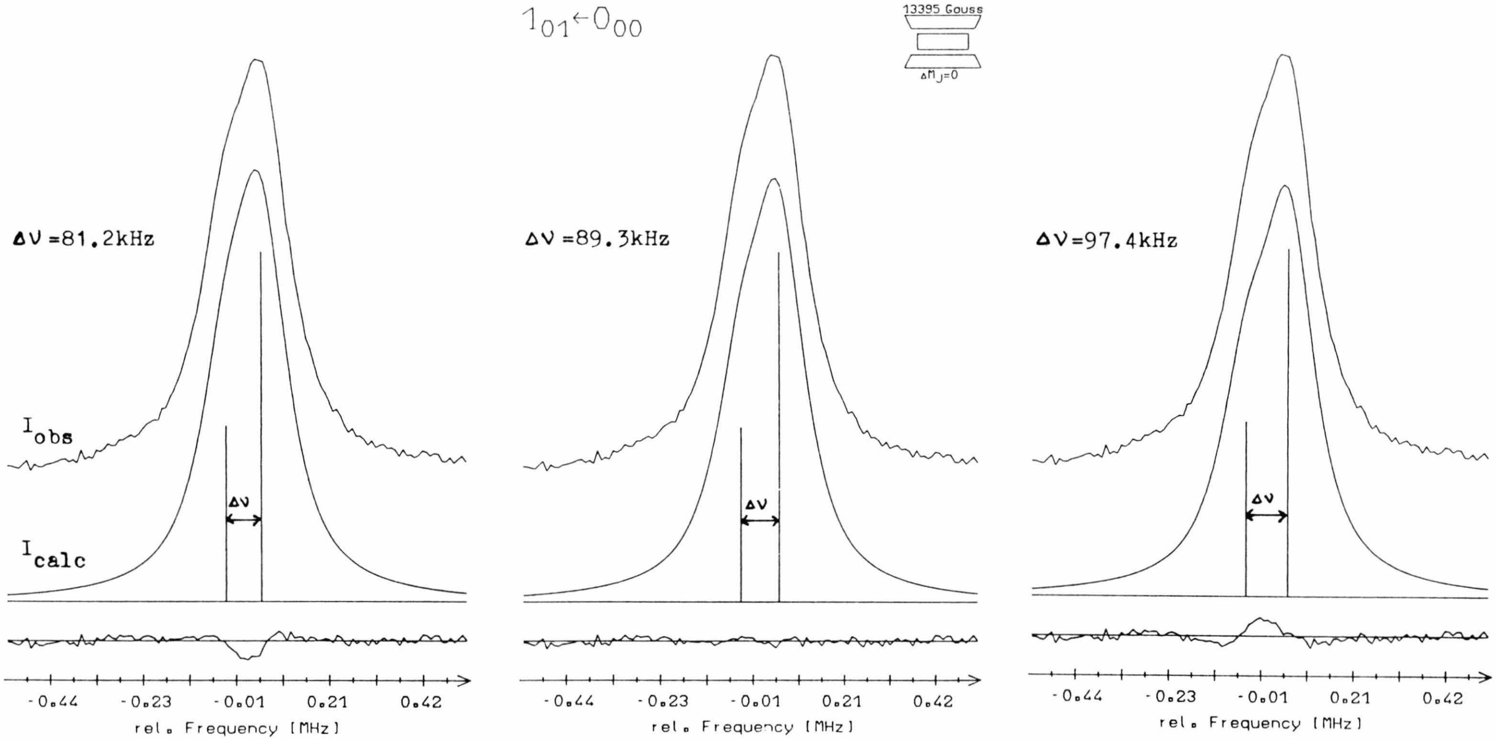

Fig. 2. Uncoupling of ^{14}N spin and overall rotation causes the $1_{01} \leftarrow 0_{00}$ rotational transition of methyl nitrate to split into a closely spaced doublet with intensity ratio 1 ($M_I=0$) to 2 ($M_I=\pm 1$). Even though the $M_I=0$ satellite only shows up as a shoulder, the splitting, $\Delta\nu=89.3\pm0.9$ kHz, follows with high accuracy from a lineshape analysis. The three pictures demonstrate the sensitivity of the difference between the observed (I_{obs}) and calculated (I_{calc}) line profile with respect to minor changes in the assumed splitting (bottom trace).

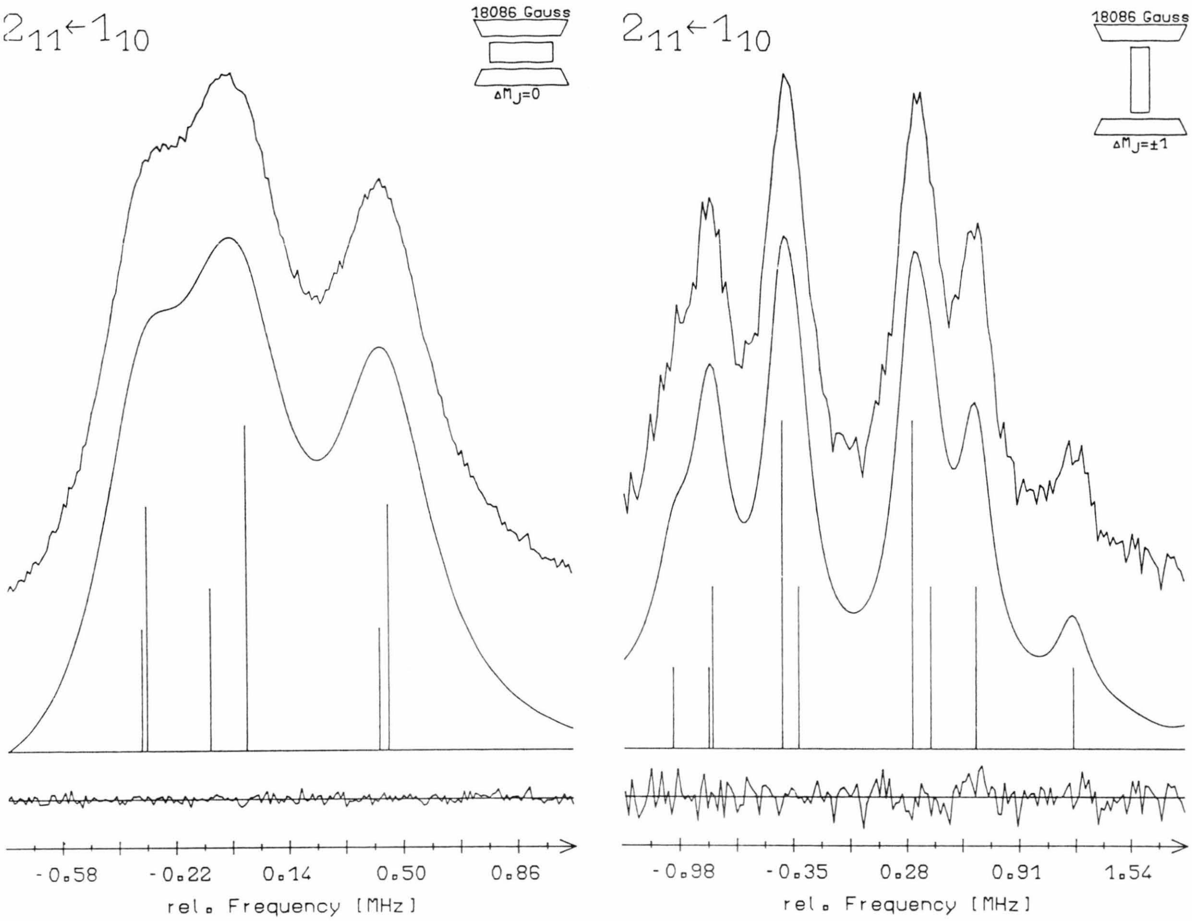

Fig. 3. Experimental and calculated Zeeman-^{14}N-hfs multiplets of the 211 ←110 rotational transition of methyl nitrate observed under $\Delta M_J = 0$ (left) and $\Delta M_J = \pm 1$ selection rule (right). As in Fig. 2 the bottom trace gives the difference between the experimental and the calculated line profile. The frequencies are given with respect to the hypothetical center frequency of the transition. For the absolute values of the frequencies compare Table 2.

The electric dipole selection rules for the rotational transitions in the strong magnetic field are either $\Delta I = 0$, $\Delta M_I = 0$, $\Delta J = 0, \pm 1$, and $\Delta M_J = 0$ (electric vector of the microwave parallel to the exterior magnetic field) or $\Delta I = 0$, $\Delta M_I = 0$, $\Delta J = 0, \pm 1$, and $\Delta M_J = \pm 1$ (electric vector of the microwave perpendicular to the exterior magnetic field). Since the electric vector of the microwave is strictly polarized perpendicular to the broad face of the waveguide cells, the proper selection rule can be choosen by the orientation of the waveguide relative to the exterior field ([8], Chapt. III,C).

The observed transitions, the magnetic fields, the rotational assignments, and the relative intensities of the satellites within each multiplet are given in Table 2. For each multiplet the satellite frequencies were determined from a least squares fit to the observed line profile. In the fitting routine the relative intensities of the satellites were used as known input. They follow by theory from the direction cosine matrix elements. Thus the fitted parameters were the satellite frequencies, the position of the baseline, one intensity, and the halfwidth. (As an approximation the same halfwidth was used for all satellites which corresponds to the assumption of identical collisional relaxation for all M_J, M_I-substates. This assumption not only leads to good fits but also appears to be reasonable in the light of recent results obtained by Haekel and Mäder [16] at our institute.)

The results of such line profile analyses and the sensitivity of the profile with respect to minor shifts of the satellite positions in the calculated spectra is demonstrated in Figs. 2 and 3. In these figures the top trace shows the observed line profile, the second trace shows the calculated line profile and the bottom trace shows the difference. In Fig. 2 we show the $1_{01} \leftarrow 0_{00}$ transition observed under $\Delta M = 0$ selection rule. In zero field this transition is split into a narrow triplet with relative intensities given by 1:5:3. In the high field Zeeman spectrum a doublet is observed with intensity ratio 1 ($M_I = 0$) to 2 ($M_I = \pm 1$), and the doublet splitting is closely related to the nuclear quadrupole coupling constant χ_{aa}. (Under neglect of the off-diagonal elements, (2) would give $\Delta \nu = 0.3\,\chi_{aa}$.) From the "observed" minus "calculated" plots shown in the figures one estimates the splittings to be determined with an accuracy of at least ±5 kHz. Indeed, the least squares fit gives a splitting of 89.3 kHz with a single standard deviation of only 0.9 kHz. This demonstrates that a careful line profile analysis of high resolution cw-spectra may yield results which are competitive with front line microwave Fourier transform results. Of course microwave Fourier transform spectroscopy [17] has opened the completely new field of rotational spectroscopy of almost nonpolar molecules, and its higher sensitivity combined with its inherent high resolution has yielded many new results for nitrogen and deuterium hyperfine coupling and high barrier internal rotation.

The least squares fitting of the Zeeman parameters and the ^{14}N quadrupole coupling constants to the observed multiplets was carried out in an iterative procedure. In each cycle the satellite splittings relative to the hypothetical unsplit zero field center frequency of the rotational transition were calculated from the molecular parameters obtained in the previous cycle. These calculated splittings together with the observed satellite frequencies were then used to derive a hypothetical unsplit zero field center frequency as intensity weighted mean. As the last step in the cycle a new set of molecular parameters was fitted to the above calculated splittings of the observed satellite frequencies with respect to this center frequency. The iteration procedure was stoped once the results had stabilized. Our final molecular parameters are listed in Table 3. Here and throughout this paper given uncertainties correspond to single standard deviations. The alternate sign for the molecular g-values can be ruled out since it leads to an unrealistic small expectation value for $\langle 0 | \sum c_\varepsilon^2 | 0 \rangle$ (see (7) below).

From the theoretical expressions for the molecular g-values and susceptibilities these Zeeman parameters and the rotational constants can be used to calculate the molecular electric quadrupole moments [18]. Additional input of the microwave structure determined by Cox and Waring [2] (see Fig. 1 and Table 4) leads to the so called paramagnetic susceptibilities and to the anisotropies in the second moments of the electronic charge distribution ((8) and (10) of [18], respectively). All these derived molecular parameters are listed in Table 5. In addition to the above values, which are determined directly from the Zeeman observables and the molecular structure an estimate for the bulk susceptibility and for the individual diagonal elements of the molecular magnetic susceptibility tensor in the principal inertia axes system can be obtained from an

Table 3. Molecular g-values, magnetic susceptibility anisotropies and ^{14}N nuclear quadrupole coupling constants in methyl nitrate, $H_3{}^{12}C^{16}O^{14}N^{16}O_2$ from the fit to the Zeeman-hfs-splittings reported in Table 2. The individual components of the quadrupole coupling tensor follow from Poissons equation $(\chi_{aa} + \chi_{bb} + \chi_{cc}) = 0$. If the ^{14}N nuclear quadrupole moment $Q = (2.05 \pm 0.05) \cdot 10^{-26}\ \text{cm}^2$ [13] is used, they lead to the second derivatives of the extranuclear contributions to the intra molecular Coulomb potential in direction of the molecular principal inertia axes as given at the bottom of the Table.

g_{aa}	$-0.1168(5)$
g_{bb}	$-0.0449(3)$
g_{cc}	$-0.0235(4)$
$2\xi_{aa} - \xi_{bb} - \xi_{cc}$	$1.24(54) \cdot 10^{-6}\ \text{erg G}^{-2}\ \text{mol}^{-1}$
$2\xi_{bb} - \xi_{cc} - \xi_{aa}$	$13.14(53) \cdot 10^{-6}\ \text{erg G}^{-2}\ \text{mol}^{-1}$
$\chi_+ = (\chi_{bb} + \chi_{cc})$	$-0.308(16)$ MHz
$\chi_- = (\chi_{bb} - \chi_{cc})$	$-0.262(30)$ MHz
$\langle \partial^2 V / \partial a^2 \rangle_{^{14}N}$	$6.21(47) \cdot 10^{16}\ \text{V cm}^{-2}$
$\langle \partial^2 V / \partial b^2 \rangle_{^{14}N}$	$-5.75(44) \cdot 10^{16}\ \text{V cm}^{-2}$
$\langle \partial^2 V / \partial c^2 \rangle_{^{14}N}$	$-0.46(04) \cdot 10^{16}\ \text{V cm}^{-2}$

Table 4. Principal inertia axes coordinates of the atoms in methyl nitrate as calculated from the r_s-structure shown in Fig. 1 of Cox and Waring [2]. In the last row we give the second moments of the nuclear charge distribution for this r_s-structure.

Atom	a [Å]	b [Å]	c [Å]
H (in plane)	2.6114	−0.7473	0.0000
H (out of plane)	1.8898	0.6411	0.8960
H (out of plane)	1.8898	0.6411	−0.8960
C	1.8339	0.0143	0.0000
O (bridge)	0.6172	−0.7510	0.0000
N	−0.5300	0.0557	0.0000
O (cis)	−0.3830	1.2514	0.0000
O (trans)	−1.5487	−0.5935	0.0000
$\sum_n Z_n g_n^2 / \text{Å}^2$	59.5163	21.2614	1.6056

Table 5. Molecular parameters which can be derived from the Zeeman-parameters in Table 3, from the experimental rotational constants, from the geometry of the nuclear frame and from the ab initio value for the out-off plane second moment of the electrons. (Q_{ab} and ξ_{ac} remain undetermined.)

Molecular electric quadrupole moments	Q_{aa}	$3.4(6) \cdot 10^{-26}$ esu cm^2
	Q_{bb}	$-4.6(6) \cdot 10^{-26}$ esu cm^2
	Q_{cc}	$1.2(10) \cdot 10^{-26}$ esu cm^2
Paramagnetic susceptibilities	ξ^{p}_{aa}	$118.14(10) \cdot 10^{-6}$ erg G^{-2} mol^{-1}
	ξ^{p}_{bb}	$279.73(14) \cdot 10^{-6}$ erg G^{-2} mol^{-1}
	ξ^{p}_{cc}	$357.40(26) \cdot 10^{-6}$ erg G^{-2} mol^{-1}
Anisotropies in the second moments of the electronic charge distribution	$\langle 0\vert \sum_i a_i^2-b_i^2 \vert 0\rangle$	37.14(14) Å^2
	$\langle 0\vert \sum_i b_i^2-c_i^2 \vert 0\rangle$	20.46(22) Å^2
	$\langle 0\vert \sum_i c_i^2-a_i^2 \vert 0\rangle$	$-57.60(21)$ Å^2
Diagonal elements of the magnetic susceptibility tensor with respect to the principal inertia axes system	ξ_{aa}	$-29.82(272) \cdot 10^{-6}$ erg G^{-2} mol^{-1}
	ξ_{bb}	$-25.85(272) \cdot 10^{-6}$ erg G^{-2} mol^{-1}
	ξ_{cc}	$-35.02(290) \cdot 10^{-6}$ erg G^{-2} mol^{-1}
Second moments of the electronic charge distribution	$\langle 0\vert \sum_i a_i^2 \vert 0\rangle$	64.8(10) Å^2
	$\langle 0\vert \sum_i b_i^2 \vert 0\rangle$	27.7(10) Å^2
	$\langle 0\vert \sum_i c_i^2 \vert 0\rangle$	7.2(03) Å^2 (ab initio value [20] with assumed uncertainty, see Text)

estimate or a reliable ab initio value for the out of plane second moment of the electronic charge distribution:

$$\begin{aligned}\langle c^2\rangle &= \langle 0|\sum_{\varepsilon}^{\text{electrons}} c_\varepsilon^2|0\rangle\\ &= \sum_{\nu}^{\text{nuclei}} Z_\nu c_\nu^2 + \frac{2mc^2}{N_A e^2}\{\xi_{cc}-\xi_{aa}-\xi_{bb}\}\\ &\quad + \frac{h}{16\pi^2 m_p}\left\{\frac{g_{cc}}{B_c}-\frac{g_{aa}}{B_a}-\frac{g_{bb}}{B_b}\right\}, \qquad (7)\end{aligned}$$

where Z_ν is the atomic number of the ν-th nucleus and m_p the proton mass.

Such an estimate can be obtained from the experimental value in HNO_3, where $\langle c^2\rangle = 4.40(13) \cdot 10^{-16}$ cm^2 was found [5], combined with the additivity rules as proposed for near planar molecules by Blickensderfer, Wang, and Flygare [19]. These rules are: 1 Å^2 for each in-plane atom of the first row of the Periodic Table as well as for each out-off-plane hydrogen, and 0.25 Å^2 for each in-plane hydrogen. Extrapolation from the HNO_3-value along these rules by adding 3 Å^2 (one for each of the two out-off-plane hydrogens and one for the carbon atom) then leads to $\langle c^2\rangle = 7.4$ Å^2. Direct application of the rules would lead to $\langle c^2\rangle = 7.25$ Å^2. In the present application we use the mean value from M. H. Palmers triple zeta bases calculations [20], which is $\langle c^2\rangle = 7.2$ Å^2, and we assume a rather conservative uncertainty of ± 0.3 Å^2 in this value, which embraces the value extrapolated from the HNO_3 result. Substituting this value into (7), solving for $(\xi_{cc}-\xi_{bb}-\xi_{aa})$ and combining the result with the experimental anisotropies from Table 3 then leads to the individual elements of the magnetic susceptibility tensor and to the bulk susceptibility. The results are

$$\begin{aligned}\xi_{aa} &= -29.82 \pm 2.72,\\ \xi_{bb} &= -25.85 \pm 2.72, \quad \xi_{\text{bulk}} = -30.23 \pm 2.54,\\ \xi_{cc} &= -35.02 \pm 2.90,\end{aligned}$$

all in units of 10^{-6} erg gauss^{-2} mol^{-1}.

The given uncertainties are calculated by gaussian error propagation from the assumed uncertainty of $\pm 0.3 \cdot 10^{-16}$ cm^2 in the estimate for $\langle c^2\rangle$ and from the experimental uncertainties of the Zeeman parameters listed in Table 3. They are largely dominated by the uncertainty assumed for $\langle c^2\rangle$, which alone adds 2.4 to 2.5 units to the final values.

Discussion

In Fig. 4 we compare ^{14}N quadrupole coupling in nitric acid [5] and in methyl nitrate. In nitric acid we had previously been able to determine the complete

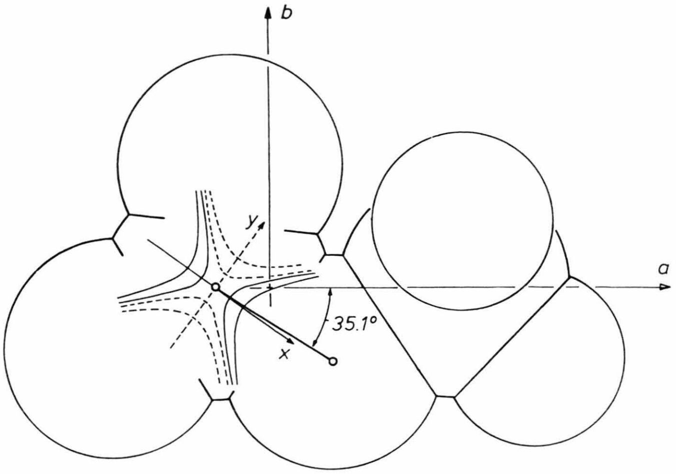

Fig. 4. ^{14}N quadrupole coupling tensor, transferred as shown from nitric acid [5] into the molecular frame of methyl nitrate, leads to coupling constants, which closely match the observed values (compare Eq. (8) of the text). The hyperbolas (not drawn to scale) correspond to isopotential curves of the Coulomb potential caused by the extranuclear charge distribution. Dashed lines indicate negative deviations from sphericity, solid lines indicate positive deviations. Quadrupole coupling probes these deviations inside the volume of the nucleus.

coupling tensor from the coupling constants in the two isotopomers $HONO_2$ and $DONO_2$. For the comparison with our present results we now assume that the electric field gradients in both molecules are identical with the x-axis of the quadrupole coupling tensor tilted by 1.1° with respect to the N–O-axis (see Figure 4). With this assumption and with the knowledge of the principal inertia axes relative to the nuclear frame from the microwave structures we are in the position to predict the quadrupole coupling constants for methyl nitrate as

$$\begin{aligned}\chi_{aa}(\text{nitrate}) &= \cos^2(\varphi)\,\chi_{xx}(\text{acid}) + \sin^2(\varphi)\,\chi_{yy}(\text{acid}),\\ \chi_{bb}(\text{nitrate}) &= \sin^2(\varphi)\,\chi_{xx}(\text{acid}) + \cos^2(\varphi)\,\chi_{yy}(\text{acid}),\\ \chi_{cc}(\text{nitrate}) &= \chi_{zz}(\text{acid}),\end{aligned} \tag{8}$$

where $\varphi = 35.1^\circ + 1.1^\circ$ is taken from the microwave structures. Substituting $\chi_{xx}(\text{acid}) = 1.103(19)$ MHz, $\chi_{yy}(\text{acid}) = -1.033(21)$ MHz and $\chi_{zz}(\text{acid}) = -0.070(8)$ MHz into (8) gives

$$\chi_{aa}^{\text{pred}}(\text{nitrate}) = +0.358 \pm 0.040,$$
$$\chi_{bb}^{\text{pred}}(\text{nitrate}) = -0.288 \pm 0.039,$$
$$\chi_{cc}^{\text{pred}}(\text{nitrate}) = -0.070 \pm 0.008,$$

as compared to our experimental values

$$\chi_{aa}^{\text{exp}}(\text{nitrate}) = +0.308 \pm 0.016,$$
$$\chi_{bb}^{\text{exp}}(\text{nitrate}) = -0.285 \pm 0.023,$$
$$\chi_{cc}^{\text{exp}}(\text{nitrate}) = -0.023 \pm 0.023,$$

all in units of MHz. (The uncertainties in the predicted values follow from the experimental uncertainties in the χ-values of nitric acid and from an assumed additional uncertainty of ±1° in the angle between the a- and the x-axis.) The good agreement between the predicted and experimental quadrupole coupling constants indicates that the electric field gradient at the nitrogen is indeed largely unaffected by H- to CH_3-substitution, at least for individual molecules in the gas phase as studied here. We therefore believe that quite in general the ^{14}N quadrupole coupling tensor of the nitrogen group as determined in [5] will be transferable also to other molecules at least as long as π electron delocalisation by double bonds can be ruled out in the close vicinity of the nitro group.

We now turn to the discussion of the magnetic susceptibility tensor. Assuming that the molecular magnetic susceptibility tensor can be constructed as a sum of local contributions, we should be able to predict the tensor of methyl nitrate from the tensor of nitric acid [5] and local tensors for H- and $C_{sp^3}(CH_3\text{-})$ determined previously. The latter values are presented in Table 6, which is an excerpt of Table II.2 of [8]. In order to minimize uncertainties we concentrate on the experimental values of the out-off-plane minus in-plane anisotopes i.e. on $2\xi_{cc} - \xi_{aa} - \xi_{bb}$. In nitric acid the experimenal value was

$$(2\xi_{cc} - \xi_{aa} - \xi_{bb})_{\text{acid}} = -7.41 \pm 0.09\,.$$

With the corresponding values for H- and CH_3- from Table 6 we predict

$$(2\xi_{cc} - \xi_{aa} - \xi_{bb})_{\text{nitrate}} = -7.41 + 0.91 + 2.56 = -3.94,$$

Table 6. Local magnetic susceptibilities for H- and C_{sp^3}- in units of 10^{-6} erg gauss^{-2} mole^{-1}. They are taken from [8], Table II.2.

$y \uparrow \rightarrow x$	ξ_{xx}	$\xi_{yy} = \xi_{zz}$
H-	$-1.17(53)$	$-2.08(38)$
C_{sp^3} (H_3C-)	$-9.92(181)$	$-8.27(149)$

all in units of 10^{-6} erg gauss^{-2} mole^{-1}. This value sharply contrasts with our experimental value

$$(2\xi_{cc} - \xi_{aa} - \xi_{bb})^{\text{exp}}_{\text{nitrate}} = -1.24(54) - 13.14(53) = -14.38(76).$$

The observed anisotropy is about 10.4 units more negative than predicted, which vastly exceeds the uncertainties normally encountered in the application of the local rules (compare for instance Table II.4 of [8]).

At present we speculate that hyperconjugation might sufficiently change the local susceptibility tensor of the methyl-group and the nitro-group. To check this, we plan to study the rotational Zeeman effect of additional molecules containing the $-ONO_2$ and $-NO_2$ groups, respectively. It would certainly also be of interest, whether an ab initio calculation such as developed by Kutzelnigg and coworkers [21] could provide some deeper understanding of the observed anomaly.

Acknowledgements

We would like to thank Dr. M. H. Palmer for many discussions on the ab initio calculations and for sending his results prior to publication.

We would also like to thank Mr. M. Andolfatto for his assistance in preparing the sample and Profs. H. Dreizler and H. Mäder for critically reading the manuscript.

Financial support by Fonds der Chemischen Industrie Deutschlands is also gratefully acknowledged.

[1] W. B. Dixon and E. B. Wilson, J. Chem. Phys. **35,** 191 (1961).

[2] A. P. Cox and S. Waring, Trans. Faraday Soc. **67,** 3441 (1971).

[3] S. S. Butcher, Ph.D. thesis, Harvard University 1962.

[4] The program FC3IAM (W. Kasten, Ph.D. thesis, Kiel 1985) an extension of the original program developed by R. C. Woods (Ph.D. thesis, Harvard University 1965) was used to calculate the internal rotation splittings.

[5] L. Albinus, J. Spieckermann, and D. H. Sutter, J. Mol. Spectrosc. **133,** 128 (1989).

[6] A. P. Black and F. H. Barbers, in: Organic Syntheses (J. R. Jonson, ed.), vol. XIX, p. 64, John Wiley & Sons, New York 1939.

[7] W. H. Stolze, Ph.D. thesis, Kiel 1988.

[8] D. H. Sutter and W. H. Flygare, Topics in Current Chemistry **63,** 89 (1976).

[9] E. C. Kemble, The Fundamental Principles of Quantum Mechanics with Elementary Applications, Chapt. 48c, Dover Publications, New York 1937.

[10] D. H. Sutter, Z. Naturforsch. **26a,** 1644 (1971).

[11] Ref. [8], Chapter IV.

[12] D. H. Sutter and W. H. Flygare, J. Amer. Chem. Soc. **91,** 6895 (1969).

[13] D. Sundholm, P. Pyykkö, L. Laaksonen, and A. J. Sadly, Chem. Phys. **101,** 219 (1986).

[14] W. Gordy and R. L. Cook, Microwave Molecular Spectra, John Wiley & Sons, New York 1984, p. 859.

[15] J. H. S. Wang and W. H. Flygare, J. Chem. Phys. **52,** 5638 (1969).

[16] J. Haekel and H. Mäder, J. Quant. Spectrosc. Radiat. Transfer **41,** 9 (1989).

[17] H. Dreizler, Mol. Phys. **59,** 1 (1986).

[18] W. Hüttner, M. K. Lo, and W. H. Flygare, J. Chem. Phys. **48,** 1206 (1968).

[19] R. P. Blickensderfer, J. H. S. Wang, and W. H. Flygare, J. Chem. Phys. **51,** 3196 (1969).

[20] M. H. Palmer, private communication.

[21] M. Schindler and W. Kutzelnigg, J. Chem. Phys. **76,** 1919 (1982).

[22] G. M. Barrow, Introduction to Molecular Spectroscopy, McGraw-Hill, Kogakusha Ltd., Tokyo 1962, p. 11.